Global J. Environ. Sci. Manage. 9(2): 241-260, Spring 2023, Serial #34

Global Journal of Environmental Science and Management
(GJESM)

Homepage: https://www.gjesm.net/

Podcasts

ORIGINAL RESEARCH PAPER

Components and predictability of pollutants emission intensity

Z. Farajzadeh[1], M.A. Nematollahi[2,*]

[1] *Department of Agricultural Economics, College of Agriculture, Shiraz University, Shiraz, Iran*

[2] *Department of Biosystems Engineering, College of Agriculture, Shiraz University, Shiraz, Iran*

ARTICLE INFO

Article History:
Received 27 June 2022
Revised 05 September 2022
Accepted 16 October 2022

Keywords:
Emission intensity
Energy
Neural network
Pollutants.

DOI: 10.22034/gjesm.2023.02.05

ABSTRACT

BACKGROUND AND OBJECTIVES: The rank of Iran in terms of pollutant emissions, which mainly originate from the consumption of energy products, is much higher than the rank of gross domestic product, placing Iran the fourth in the production and consumption of gas and oil, among the cases with the highest emission intensity in the world. Different driving forces account for the high emission intensity. This study decomposes the changes in the aggregate emission intensity of the selected pollutants into a broader scope of driving forces including energy, urbanization, output, labor, and trade-related variables. The examined pollutants were far beyond carbon dioxide, including nitrogen oxides, sulphur dioxide, and carbon monoxide, emitted from energy product consumption. The aim of this study was to investigate the emission intensity of the selected pollutants and their components.

METHODS: Decomposition analysis was done to decompose the emission intensity into a broader scope of the driving forces far beyond what examined in the literature. For this purpose, two well-known artificial neural networks, multilayer perceptron, and wavelet-based neural network were applied to forecast the emission intensity of the selected pollutants and their components.

FINDINGS: The emission intensity of nitrogen oxides and sulphur dioxide illustrated a decreasing trend. In contrast, a general increasing trend with significant fluctuation was observed for carbon monoxide and carbon dioxide emission intensity. Among the components, energy structure, population-labor ratio, and trade openness showed an intensity decreasing effect, while urban per capita output, urbanization, energy intensity, and industrial output-trade ratio contributed to higher emission intensity of the pollutants. Moreover, the multilayer perceptron and wavelet-based neural networks were recommended to examine the predictability of the emission intensity and its components.

CONCLUSION: It was found that intensive and extensive growth and energy structure were the most significant driving forces of the emission intensity. The forecast results indicated that the emission intensity of nitrogen oxides, sulphur dioxide, and carbon monoxide might be predicted by the applied networks with a prediction error of less than 0.2 percent. However, the prediction error for carbon dioxide emission intensity was much higher.

NUMBER OF REFERENCES	NUMBER OF FIGURES	NUMBER OF TABLES
54	10	2

*Corresponding Author:
Email: *manema@shirazu.ac.ir*
Phone: +9871 3613 8382
ORCID: 0000-0001-5780-2723

Note: Discussion period for this manuscript open until July 1, 2023 on GJESM website at the "Show Article".

INTRODUCTION

Global carbon dioxide (CO_2) emissions increased by 1.9 percent (%) annually over 1990-2016, while the corresponding figure for production was 3.2% (World Bank, 2016), indicating a decreasing trend in CO_2 emissions intensity. However, regarding the role of greenhouse gases (GHGs) in climate change (Naderipour *et al.*, 2020), more efforts are needed to lower the emission intensity. Emission mitigation has received more attention after the Paris Agreement in 2015, leading to a reinforcement of developing countries' involvement (Rodríguez and Pena-Boquete, 2017). Accordingly, Iran intends to abate its GHGs emissions to 4% below baseline by 2030, having the potential of an additional 8% (UNFCCC, 2015). Globally, about 65% of the GHGs are emitted from the production and use of energy (Marrero, 2010). The corresponding figure for Iran is over 80% (Farajzadeh, 2018). Despite the global attempts to diminish the energy intensity, it has been increasing in Iran over decades (Farajzadeh and Nematollahi, 2018). Iran, as the 8th biggest CO_2 emitter in the world (World Bank, 2018a), is ranked the 18th in terms of gross national income (GNI) based on purchasing power parity (PPP) (World Bank, 2019), indicating its higher emission intensity compared to the world. The CO_2 emission intensity of Iran is around 0.56 kg, which is more than twice the world's emission intensity (World Bank, 2018b). To the best of authors' knowledge, the increasing intensity of emissions and their driving forces have not received adequate attention in Iran. Although the CO_2 emission is more important since it plays a central role in global warming (Böhringer and Löschel, 2006), other GHGs such as methane (CH_4), and nitrous oxide (N_2O), acidifying substances such as sulphur dioxide (SO_2), and nitrogen oxides (NO_x), and health-damaging pollutants such as carbon monoxide (CO) are also important (Farajzadeh *et al.*, 2017). These pollutants are highly important in the Iranian economy, which is ranked the fourth in the production and consumption of gas and oil in the world (Farajzadeh, 2018). The estimated energy-related emissions of CO_2, NO_x, SO_2, and CO in 2018 have been equal to 635.2, 2.05, 0.82, and 11.75 million tons, respectively (Iran's Energy Balance, 2018). Considering the medium damage costs (World Bank, 2004), around 43.7% of total damage caused by the selected pollutants are related to NO_x, SO_2, and CO, and the remaining share pertains to CO_2. In other words, in terms of damage cost, other pollutants are also extremely important. Although energy intensity is an important factor in emission intensity, there is a great room for further progress in examining other driving forces, including output structure, urbanization, industrialization, and energy composition (Rodríguez and Pena-Boquete, 2017; Zhang *et al.*, 2019). The decomposition technique is a tool that can help in examining the possible variables affecting the emission intensity. Attempts to examine the emissions intensity have been increasing over the last decade. Xu and Ang (2013) believed that a few studies examined the emission intensity. Accordingly, Steckel *et al.* (2011) suggested to decrease the energy intensity in order to reduce the emissions and especially carbon intensity in China. A similar result was also found by Cheng *et al.* (2014). Rodríguez and Pena-Boquete (2017) suggested that higher output stemming from increased labor productivity led to lower carbon intensity in Asian Dragons countries, while an increase in industrial energy use per worker contributed to the reverse direction. Dong *et al.* (2018) reported the negative effect of per capita gross domestic product (GDP) on Chinese carbon emission intensity. In the same vein, Zhang and Hao (2020) found a negative relationship between SO_2 and chemical oxygen demand (COD) intensities and per capita GDP in Chinese provinces. Han *et al.* (2019) found that 1% increase in GDP resulted in 2.61% increase in carbon emission intensity in China. GDP was also found as the main driving force for carbon intensity among the countries membered in the Organization for Economic Cooperation and Development (OECD) (Pan *et al.*, 2019). Although the economy's structure is mainly examined using output composition or industrial output share, as discussed by Farajzadeh and Nematollahi (2018), urbanization may also reveal the level of economic development. Similar to the income effect, both positive and negative effects have been highlighted for urbanization. For example, some empirical works showed that urbanization could lead to negative environmental consequences (Lean and Smyth, 2010; Mishra *et al.*, 2009), which is mainly assigned to more energy-intensive activities (Holtedahl and Joutz, 2004). On the other hand, urbanization may make it possible to enjoy economies of scale and more efficient use of energy (Jones, 1991). Dong *et al.* (2018) and Han *et al.* (2019) reported the dampening

effect of urbanization on carbon intensity in China. In a different view, it was suggested that the impact of urbanization depended on the level of economic development (Sadorrsky, 2013). However, as implicitly declared by Naderipour *et al.* (2021), urban services include emissions. As for energy intensity, goods-producing and industrial activities are expected to raise energy intensity (Poumanyvong and Kaneko, 2010; Adom, 2015), leading to higher emissions as well. Dong *et al.* (2018) showed that more industrialization of China's economy might be accompanied by higher carbon intensity. However, there is an evidence for energy intensity reduction (Adom and Kwakwa, 2014) and even emissions-reducing effects of industrialization (Zhang *et al.*, 2019). Other components of emission intensity are emission coefficient factor, employment, and energy structure (mix). Zhang *et al.* (2019) reported an emissions-reducing effect for the emission coefficient in China. However, Rodríguez and Pena-Boquete (2017) and Han *et al.* (2019) found a positive relation between this variable and carbon intensity in China. The emission intensity reducing effect of urban employment was found to be enormously significant in China (Han *et al.*, 2019). Similarly, Zhang and Hao (2020) and Long *et al.* (2015) reported a positive impact of unemployment on SO_2 emissions intensity and carbon emissions in China, respectively. There is also an evidence for positive impact of energy mix on carbon intensity (Dogan and Seker, 2016; Dong *et al.*, 2018). There is a great body of literature indicating the significant role of trade openness in energy intensity. The energy intensity reducing effect of trade openness has been suggested for Nigeria (Adom, 2015), Chinese provinces (Herrerias *et al.*, 2013), and emerging economies (Rafiq *et al.*, 2016). However, Shahbaz *et al.* (2019) found that for the United States, trade openness decreased the CO_2 emissions, while foreign direct investment (FDI) adversely affected it. The CO_2 emission increasing role of FDI or trade has been reported for the emerging economies such as Malaysia (Lau *et al.*, 2014), Tunisia (Shahbaz *et al.*, 2014), Brazil, China, Egypt, Mexico, Nigeria, and South Africa (Onafwora *et al.*, 2014). The contribution of the present study to the current literature is fourfold. First, it extends the index decomposition analysis using a broader scope of the driving forces far beyond what examined in the literature. Second, the decomposition of pollutants is extended beyond CO_2 to SO_2, NO_x, and CO. Third, the relevance of the applied components as driving forces in the emissions intensity determination is evaluated. Fourth, the multilayer perceptron (MLP) and the wavelet-based neural networks (WNNs) are designed for all components individually, in which a set of economic determinants are applied. The distinguishing feature of WNNs is that they use a class of functions named "wavelets". The objective of the current study was to examine the components of the selected pollutants' emission intensity. Moreover, a time series covering the period of 1988-2018 was applied as the required data. This study was carried out in Iran in 2020.

MATERIALS AND METHODS

Decomposition method

Decomposition analysis is widely used to identify the driving forces affecting energy consumption and environmental deterioration (Ang and Zhang, 2000; Su and Ang, 2012). There are two major decomposition techniques, i.e., index decomposition analysis (IDA), and structural decomposition analysis (SDA). Generally, IDA is easier to be empirically used compared to SDA (Zhang *et al.*, 2019). IDA approach enjoys various formulations and applications. These methods can be divided into Laspeyres and Divisia families (Ang, 2015; Zhang *et al.*, 2019). The log mean Divisia index (LMDI) method in the Divisia family, which is preferred to other methods (Greening *et al.*, 1997; Ang, 2004), has been broadly used to decompose CO_2 emissions for its advantages in working with the remaining items and zero values (Ang, 2015). It should be noted that the LMDI technique has been adopted in this study. Following the index decomposition method, the emission intensity of the selected pollutants was expressed using Eq. 1 (Rodríguez and Pena-Boquete, 2017; Zhang *et al.*, 2019).

$$P^k = \sum_i \sum_j P_{ij}^k = \sum_i \sum_j \frac{P_{ij}^k}{E_{ij}} \times \frac{E_{ij}}{E_i} \times \frac{E_i}{Y_i} \times \frac{Y_i}{Y} \times \frac{Y}{P} \times P \quad (1)$$

Where, P^k is total amount of *k*th pollutant emissions; P_{ij}^k is amount of *k*th pollutant emitted in production sector *i* by fuel j; E_{ij} is a mount of *j*th energy product consumed in production sector *i*; E_i is total energy products used in production sector *i*; Y_i is output of sector *i*; Y is total output; P is total

population; $\frac{P_{ij}^k}{E_{ij}}$ is *k*th pollutant emission coefficient of energy product *j* in sector *i*; $\frac{E_{ij}}{E_i}$ is the share of *j*th energy product in total energy use of sector *i* (energy structure or energy mix including gasoline, kerosene, fuel oil, gas oil, liquid gas, natural gas, and electricity); $\frac{E_i}{Y_i}$ is energy intensity in sector *i* (sectoral energy intensity); $\frac{Y_i}{Y}$ is the output share of sector *i* in total output (economic structure), and $\frac{Y}{P}$ is per capita output (income).

The emission intensity of pollutant *k* was calculated using Eq. 2 (Zhang *et al.,* 2019).

$$PI^k = \frac{P^k}{Y} = \sum_i \sum_j \frac{P_{ij}^k}{E_{ij}} \times \frac{E_{ij}}{E_i} \times \frac{E_i}{Y_i} \times \frac{Y_i}{Y} \times \frac{Y}{P} \times P \times \frac{1}{Y} \quad (2)$$

GDP growth can be attributed to the extensive use of resources and higher productivity. By multiplying Eq. 2 by L/L, the above-mentioned sources of GDP growth could be obtained using Eq. 3 (Rodríguez and Pena-Boquete, 2017).

$$PI^k = \frac{P^k}{Y} = \sum_i \sum_j \frac{P_{ij}^k}{E_{ij}} \times \frac{E_{ij}}{E_i} \times \frac{E_i}{Y_i} \times \frac{Y_i}{Y} \times \frac{Y}{P} \times \frac{P}{L} \times \frac{L}{Y} \quad (3)$$

Where, $\frac{P}{L}$ is the *inverse of employment* rate and $\frac{L}{Y}$ is the *inverse of labor productivity*. The former element shows the extensive use of labor (extensive growth), and the latter examines the intensive nature of economic growth. The index decomposition was extended using urbanization, industrialization, and trade openness as expressed using Eq. 4 (Li *et al.,* 2017; Zhang *et al.,* 2019).

$$PI^k = \frac{P^k}{Y} = \sum_i \sum_j \frac{P_{ij}^k}{E_{ij}} \times \frac{E_{ij}}{E_i} \times \frac{E_i}{Y_i} \times \frac{Y_i}{U} \times \frac{U}{P} \times \frac{P}{L} \times \frac{L}{Y} \times \frac{Y}{M} \times \frac{M}{T} \times \frac{T}{Y} \quad (4)$$

Where, $\frac{Y_i}{U}$ is the output of sector *i* – urban population ratio; $\frac{U}{P}$ is urbanization; $\frac{Y}{M}$ is the GDP-industrial output ratio or the *inverse of industrialization*; $\frac{M}{T}$ is the industrial output-trade ratio; and $\frac{T}{Y}$ is trade openness (*economic integration*). Applying the logarithmic mean weighting scheme, the emissions intensity components could be presented by Eq. 5 (Ang, 2015; Zhang *et al.,* 2019).

$$\Delta PI^k = \Delta PE^k + \Delta EE + \Delta EY + \Delta YU + \Delta UP + \Delta PL + \Delta LY + \Delta YM + \Delta MT + \Delta TY \quad (5)$$

Emissions intensity changes from the base year 0 to target year *t* could be decomposed using Eq. 6 (Ang, 2015).

$$\begin{aligned}\Delta PI^k &= PI_t^k - PI_0^k \\ &= \sum_{ij} L_{ij} \cdot ln\frac{PE_{ij.t}^k}{PE_{ij.0}^k} + \sum_{ij} L_{ij} \cdot ln\frac{EE_{ij.t}}{EE_{i.0}} + \sum_{ij} L_{ij} \cdot ln\frac{EY_{i.t}}{EY_{i.0}} + \\ &\sum_{ij} L_{ij} \cdot ln\frac{YU_{i.t}}{YU_{i.0}} + \sum_{ij} L_{ij} \cdot ln\frac{UP_t}{UP_0} \\ &+ \sum_{ij} L_{ij} \cdot ln\frac{PL_t}{PL_0} + \sum_{ij} L_{ij} \cdot ln\frac{LY_t}{LY_0} + \sum_{ij} L_{ij} \cdot ln\frac{YM_t}{YM_0} + \\ &\sum_{ij} L_{ij} \cdot ln\frac{MT_t}{MT_0} + \sum_{ij} L_{ij} \cdot ln\frac{TY_t}{TY_0}\end{aligned} \quad (6)$$

Where, $L_{ij} = \left(PI_{ij.t} - PI_{ij.0}\right) / \left(lnPI_{ij.t} - lnPI_{ij.0}\right)$ for $PI_t \neq PI_0$ and $L_{ij} = PI_{ij.t}$ when $PI_t = PI_0$.

Artificial neural network model

In this study, two well-known artificial neural networks (NNs), multilayer perceptron (MLP), and wavelet-based neural network (WNN) were employed to forecast the emission intensity and its components for the selected pollutants. The NNs include some interconnected computing elements (neurons) inspired by the biological brain. The feed-forward type is a topology widely used in the NNs structure for many applications in engineering and science, such as forecasting (Fig. 1). The aim of the learning process is to adjust the weights and biases in the NNs structure, while an error function in the output layer is minimized using Eq. 7 (Nematollahi *et al.,* 2012).

$$E = \sum_{k=1}^{K} \left[(EI_M)_k - (EI_P)_k \right]^2 \quad (7)$$

Where, EI_M is the observed (target) data presented to the NNs as input; EI_P is predicted by the NNs, including the weights and biases; and *K* denotes the number of outputs. To adjust the weights, the back-propagation (BP) as an iterative algorithm was employed using Eq. 8 (Nematollahi *et al.,* 2012).

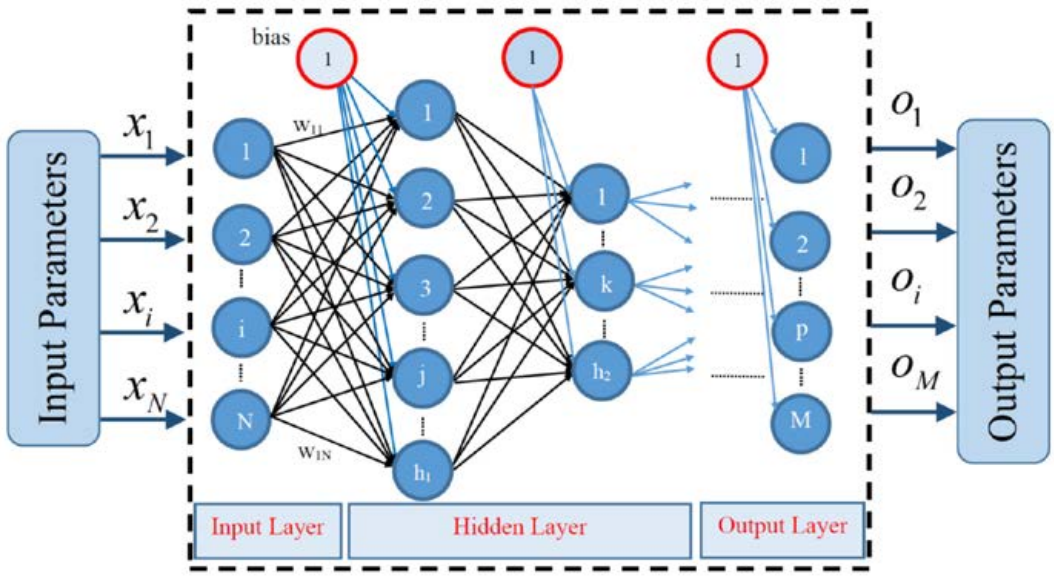

Fig. 1: Structure of the MLP-feedforward network

$$w_{ji}(k+1) = w_{ji}(k) + \Delta w_{ji}(k) \quad (8)$$

The generalized delta learning rule is usually used to compute $\Delta w_{ji}(k)$. Details of the structures and training algorithms of the NNs are presented in Fig. 1 (Rojas, 1996; Nematollahi *et al.,* 2020; Nematollahi and Mousavi Khaneghah, 2019).

The wavelet-based neural network (WNN)

WNN consists of a class of localized basis functions, namely wavelets. The useful features of wavelets are orthonormality, fast implementation, and locality in time and frequency (Daubechies, 1992; Mallat, 1989). A multi-resolution framework was developed by Mallat (1989), in which any function $F(\mathbf{X}) \in \mathrm{L}^2(\mathrm{R})$ could be approximated by wavelets as the basis functions using Eq. 9 (Nematollahi *et al.,* 2012).

$$\mathbf{F}(\mathbf{X}) = \sum_{k=-\infty}^{+\infty} a_{0,k}\varphi_{0,k}(\mathbf{X}) + \sum_{m=-\infty}^{0}\sum_{k=-\infty}^{k=+\infty} d_{m,k}\psi_{m,k}(\mathbf{X}) \quad (9)$$

Where, $\varphi_{0,k}$ and $\psi_{m,k}$ denote the scaling and wavelet functions, respectively; and $a_{0,k}$ $d_{m,k}$ denote an approximation and detail coefficients, respectively. These coefficients are determined using discrete wavelet transform (DWT). Fig. 2 presents two types of wavelet and their corresponding scaling functions.

The WNN training

The original time series for training the NNs initially pass through two filters and are decomposed into low (approximations) and high-frequency (details) portions (Fig. 3a and 3b).

One signal could be decomposed into lower resolution using multiple-level decomposition (Fig. 3b). Next, the NN was trained with the above-mentioned coefficients. The NN output, after training, was used to reconstruct the approximated signal as compared to the original signal (Fig. 4). To improve the performance of the NN, the training data were normalized.

To examine the accuracy of the predicted values, root mean squared error (RMSE), mean absolute error (MAE), mean absolute percentage error (MAPE), and Theil Inequality coefficient were applied.

Data

The time series related to the aggregate emissions intensity index of the selected pollutants and their components were applied as the data. The data related to the intended period (1988-2018) were obtained from the Central Bank of Iran (2018),

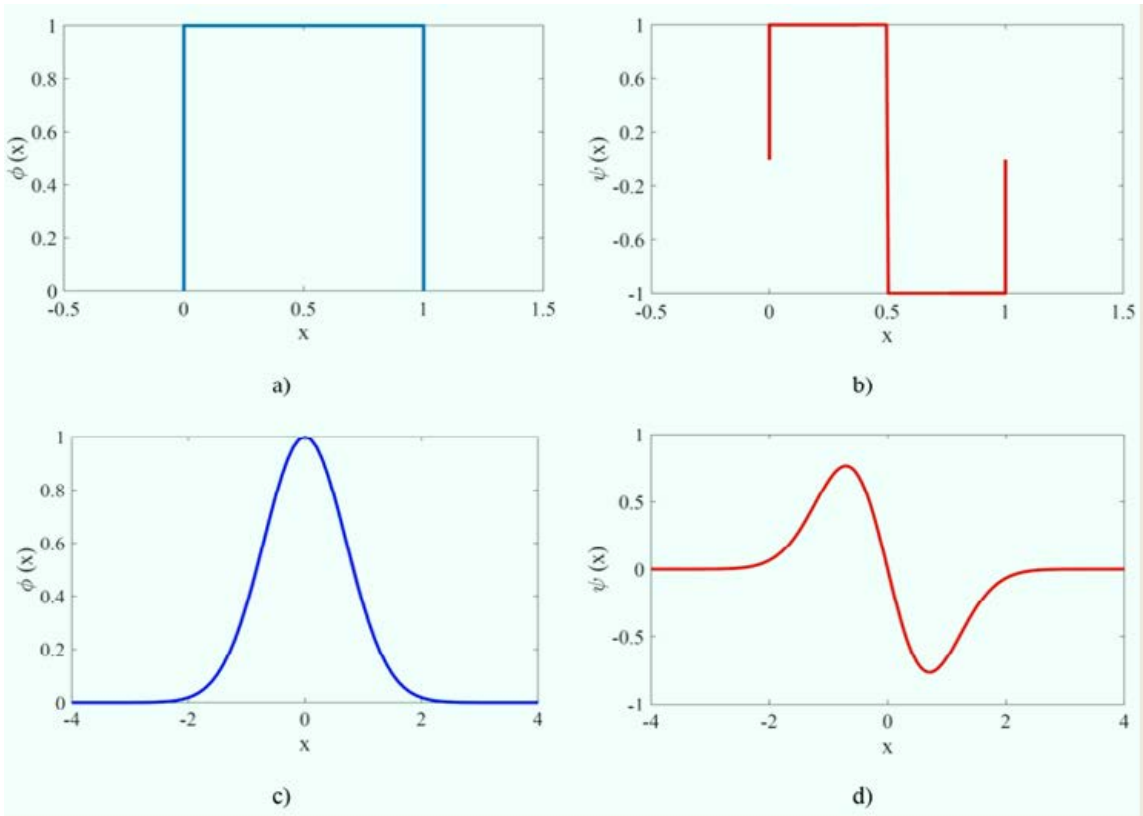

Fig. 2: Two types of wavelet and their corresponding scaling functions: a) Haar scaling function; b) Haar wavelet function; c) Gaussian scaling function; d) Gaussian wavelet function

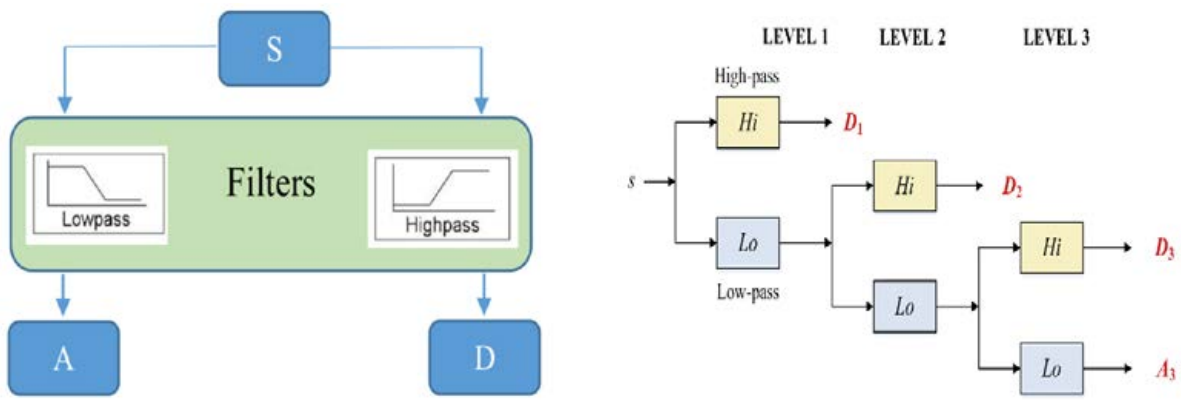

(a) (b)

Fig. 3: a) Transformation of a discrete wavelet into approximation (A) and detail (D) segments; and b) multi-level decomposition of a signal at level 3

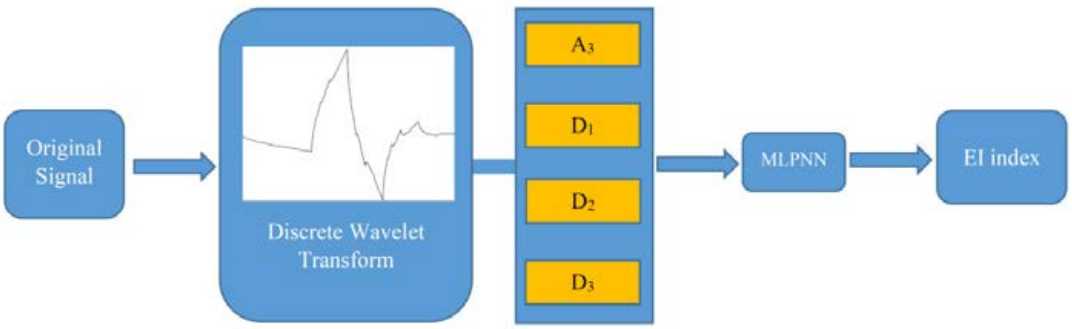

Fig. 4: The schematic structure of the wavelet neural network models

Table 1: Descriptive statistics of the selected pollutants

Pollutants	Average emission intensity	Growth of intensity (%)	Coefficient of variation	Correlation coefficients			
				NO_x	SO_2	CO	CO_2
NO_x	3.05	-0.59	0.06	1.00	0.88	-0.15	0.61
SO_2	3.24	-4.34	0.31	-	1.00	-0.39	0.23
CO	16.66	0.86	0.11	-	-	1.00	0.03
CO_2	765.10	-0.03	0.05	-	-	-	1.00

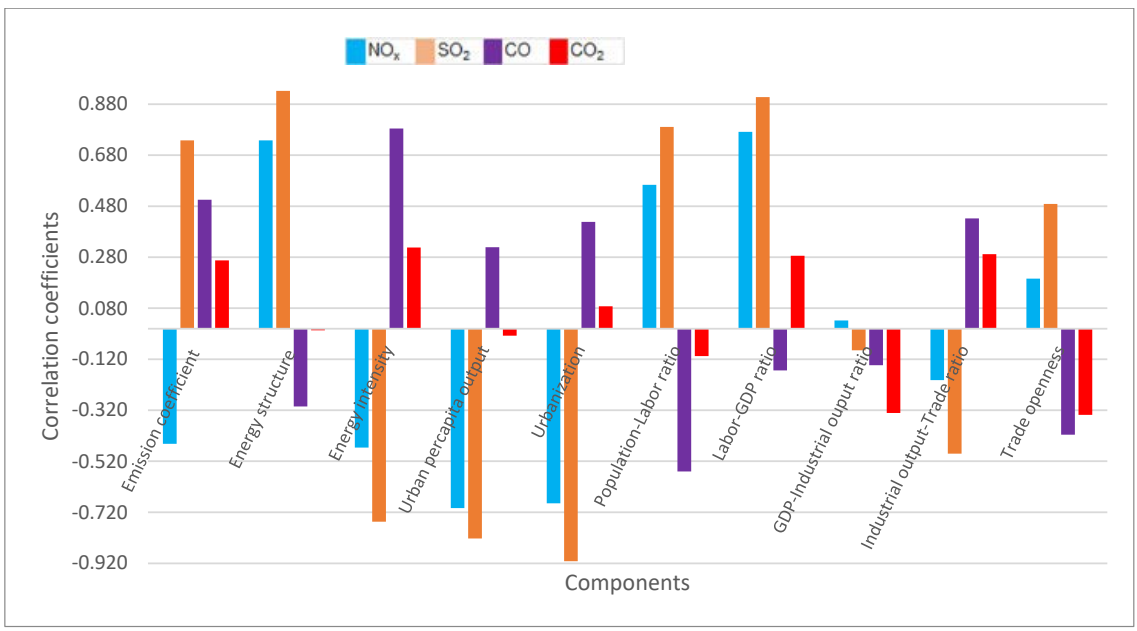

Fig. 5: Correlation coefficients of the components and emission intensity

the Statistical Center of Iran (2018), and Iran's Energy Balance (2018). Subsequently, the data were examined for the selected pollutants including NO_x, SO_2, CO, and CO_2. In NN models, data of 1988-2016 were applied for training and the data of the last two years were used for the forecast evaluation.

RESULTS AND DISCUSSION

Results of emissions intensity

Table 1 presents the descriptive information about the selected pollutants. The emission intensity of SO_2 and NO_x decreased over the study horizon by 4.34% and 0.59%, respectively. This was mainly due to the reduction in fuel oil consumption as the main origin of SO_2 and NO_x emissions. CO_2 emission intensity did not show significant changes, while CO emission intensity increased by 0.86% annually. Gasoline plays a central role in CO emissions, accounting for around 97% of emissions (Iran's Energy Balance, 2018), and the continuing growth of gasoline consumption resulted in CO emission growth. In terms of average emission intensity, CO_2 is tremendously different from other pollutants. However, considering the health damage associated with emissions, the total damage of NO_x, SO_2 and CO was comparable with that of CO_2. Higher fluctuations in SO_2 and CO emissions intensity were mainly due to fuel oil consumption. The dominant role of gasoline in CO emission was the main reason for negativity or insignificance of the correlation between CO coefficient and other pollutants (less than 0.4 in absolute value). Gas oil and gasoline were also responsible for NO_x, CO_2, and SO_2 emissions, resulting in positive and higher correlation coefficients ranging from 0.23 to 0.88. It should be mentioned that natural gas is the main source of CO_2 emission (Iran's Energy Balance, 2018).

The decomposition results of the selected pollutants are presented in Figs. 6-9. Considering the large number of components and pollutants examined, the correlation coefficients of the components and the emission intensity are presented in Fig. 5. As explained by Eq. 6, the changes in emission intensity were decomposed into ten components as influencing factors. It should be noted that the

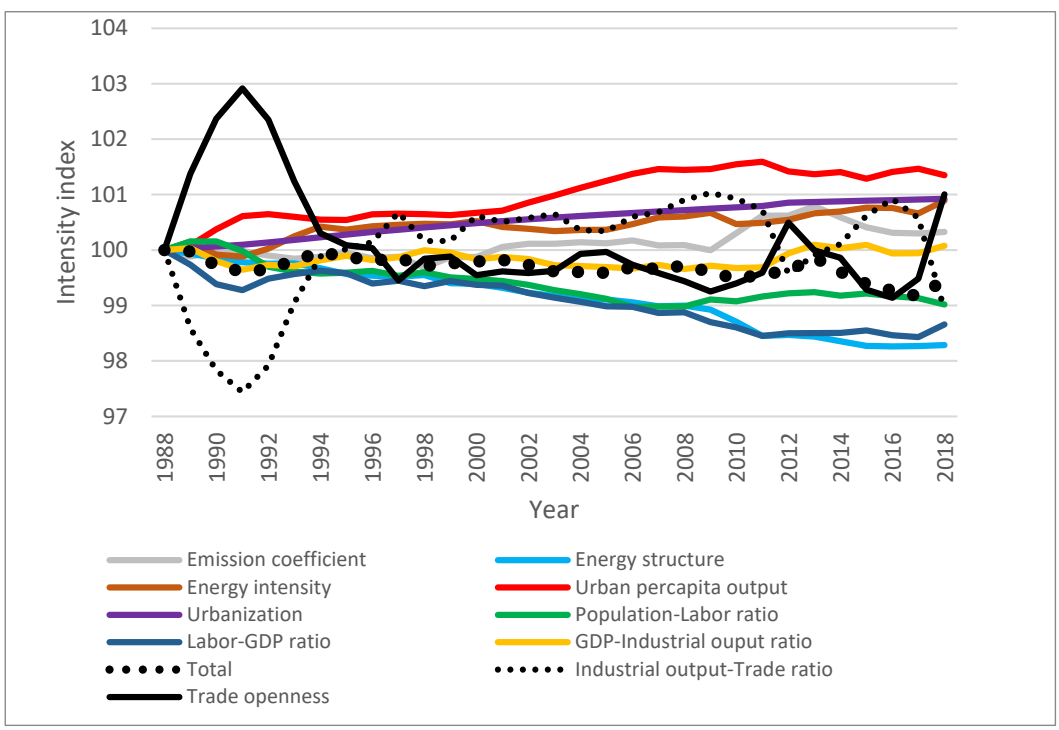

Fig. 6: NO_x emission intensity and its components

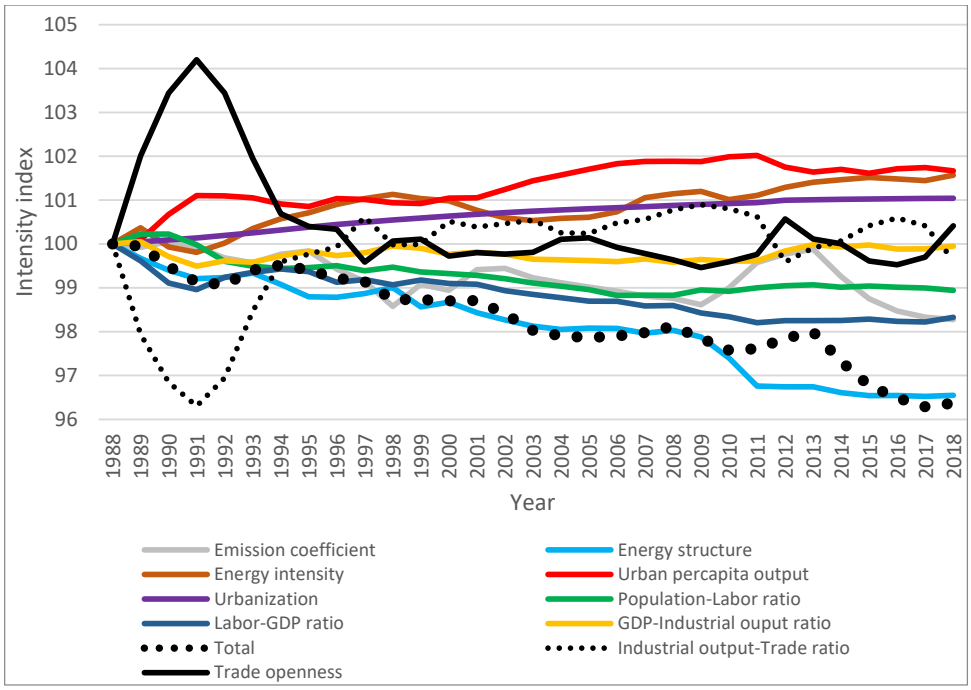

Fig. 7: SO_2 emission intensity and its components

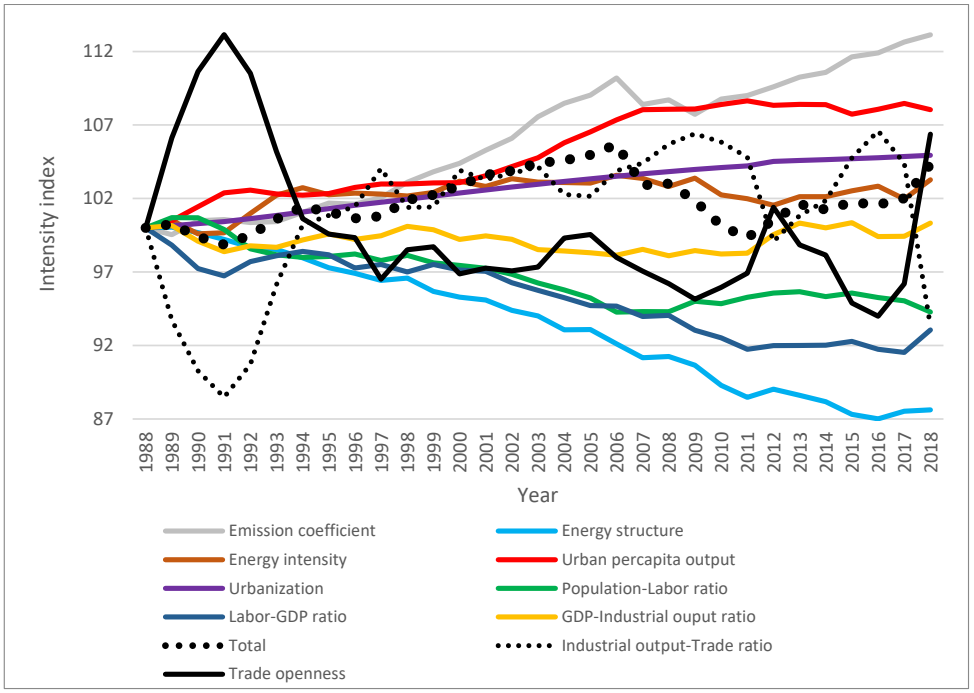

Fig. 8: CO emission intensity and its components

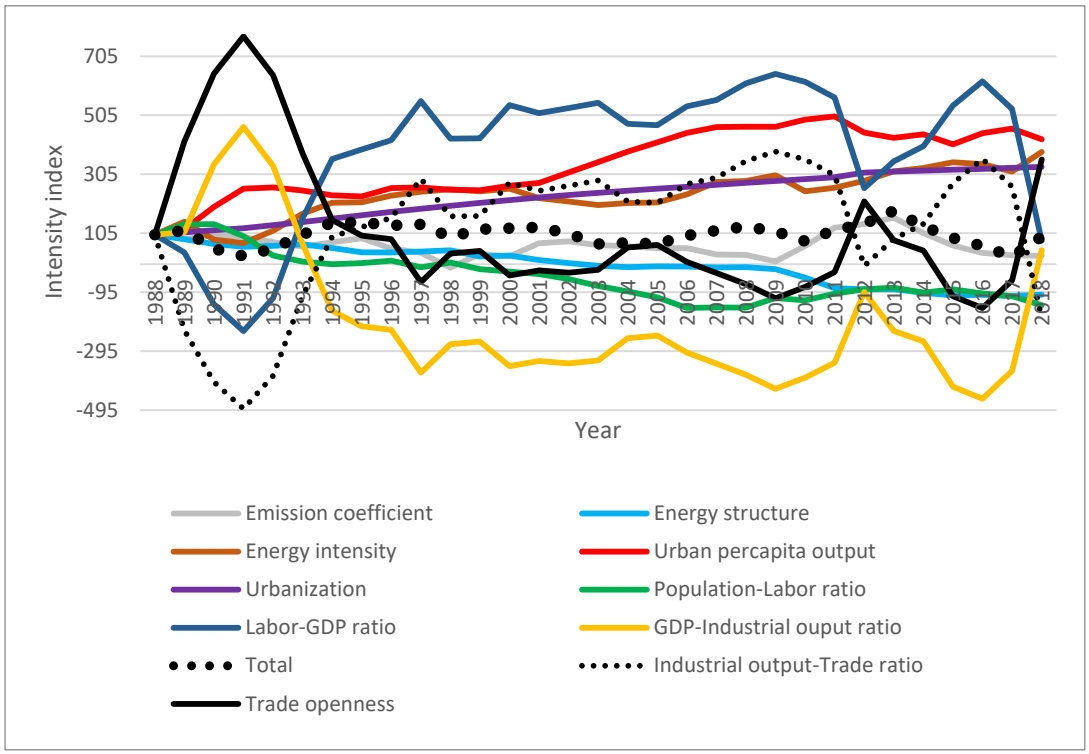

Fig. 9: CO_2 emission intensity and its components

changes in each component and emission intensity are presented in an index format starting from 100 for the base year of 1988. This allowed for observing the changing trend of the influential factors over the study horizon.

Although most of the components had a similar direction of correlation, a higher similarity was observed between NO_x and SO_2 emissions. This also applied to CO and CO_2. Thus, the results of NO_x and SO_2 were discussed together. It should be noted that the common sources of NO_x and SO_2 emissions are gasoline and gas oil, so that over 56% of NO_x and more than two-thirds of SO_2 are emitted from these products. As for CO and CO_2, gasoline and natural gas play a central role in CO and CO_2 emissions, respectively. However, in this study, gasoline and natural gas consumptions were significantly correlated, resulting in similar behavior of CO and CO_2 emissions intensity components (Iran's Energy Balance, 2018).

NO_x and SO_2 emissions intensity components

As shown in Figs. 5 and 6 and 7, there are marked similarities between the results found for NO_x and SO_2. Comparison of the results of NO_x and SO_2 components revealed some points: 1) the total emission intensity of NO_x and SO_2 showed a decreasing trend. However, a steeper trend was observed for SO_2 emissions intensity. 2) only two components (i.e., emissions coefficient, and GDP-industrial output ratio) illustrated a different direction of correlation. Since the emission coefficient reduced the emission intensity of NO_x, it was expected to contribute to higher emission intensity of SO_2 with a significant correlation coefficient as high as 0.74. The reverse order was observed for the GDP-industrial output ratio. However, the magnitude of the coefficients for this component was not significant as it was less than 0.10 in absolute value. 3) the magnitude of the correlation coefficients related to the remaining components of SO_2 was higher than that of the

correlation coefficients related to the components of NO_x. Most of the correlation coefficients for SO_2 were over 70% and for NO_x were less than 70%. During the study period, the contribution of energy products to NO_x emissions changed in favor of natural gas, while the contribution of energy products to SO_2 emissions did not experience a significant change. Considering the decreasing trend of NO_x and SO_2 emissions intensity, a positive correlation implied the reducing effect of emission intensity and vice versa. The components could be classified into three groups in terms of correlation coefficients. The first group included the components that were positively correlated with emission intensity, revealing a decreasing trend similar to the total emission intensity. The inverse labor productivity (Labor-GDP ratio), energy structure, population-labor ratio, and trade openness could be categorized in this group. The reduction in emission intensity due to energy structure changes probably occurred via a change in energy consumption toward the products that contained less NO_x and SO_2 such as liquid gas, kerosene, and even gasoline. The importance of energy composition was also pointed out by Rodríguez and Pena-Boquete, (2017) and Zhang *et al.* (2019). The second group included the components that contributed to higher emission intensity, including urban per capita output, urbanization, energy intensity, and industrial output-trade ratio, which revealed negative correlations. The third group included the emissions coefficient, and GDP-industrial output ratio that were discussed above.

Among the emission intensity-increasing components, urban-related components had the highest contribution as their correlation coefficients tended to be around 0.70 for NO_x and 0.82-0.91 for SO_2. This implicitly meant that while urbanization was expected to be accompanied by more energy use, it entailed a higher output, resulting in lower energy intensity and indicating the economies of scale as suggested by Sadorrsky, (2013). Another urban-related variable was urban per capita output or GDP-urban population ratio, which had the highest contribution to NO_x emission intensity. For SO_2, this variable, with a high correlation coefficient of 0.82, was ranked after urbanization. Urbanization was expected to be accompanied by a higher output as well. Urbanization was correlated with the output expansion in the services sector, in which the activities were more energy and pollution intensive. The correlation between the services sector output and urbanization was found to be 0.94 over 1967-2018 (Central Bank of Iran, 2018). Energy intensity was the next component inducing higher emission intensity with correlation coefficients of 0.47 and 0.76 for NO_x and SO_2, respectively. There is evidence of emission decreasing effect (Zhang *et al.,* 2019) expected to dampen the emission intensity. However, the emission intensity-raising effect of this component, to a great extent, could be attributed to the production technology. Farajzadeh *et al.* (2017) have also suggested that production processes in Iran are not highly technology-embodied ones. Additionally, sanctions might be responsible for a part of such recession in technology, since Iran has faced sanctions for many years (Hufbauer *et al.,* 2012). Energy plays a central role in the Iranian economy. In the study period, while GDP has been growing by 4.1% annually, the corresponding value for energy was obtained as 5.2%. Particularly, the consumption of natural gas (as a great source of emissions for NO_x) in the industrial and services sectors has increased by 10.8% and 11.4% annually, respectively (Iran's Energy Balance, 2018). Contrary to the role of energy intensity in raising the emission intensity, energy structure indicated that changes in energy mix would have an emission-reducing effect as already mentioned. The data showed that the energy composition changed in favor of natural gas and electricity, while the oil products share (accounting for most of the NO_x emissions in the energy basket) decreased. Zhang *et al.* (2019) also pointed out that emissions fading role of energy mix changed in favor of natural gas and electricity. Both labor-related components were positively correlated with NO_x emission intensity with correlation coefficients of higher than 0.56. In other words, these variables contributed to lower emissions intensity. Over the study horizon, population-labor and labor-GDP ratios would be decreased. In other words, an increase in employment and labor productivity would be associated with lower emission intensity. In terms of correlation coefficients (0.77 and 0.91 for NO_x and SO_2, respectively), labor productivity showed a high contribution to the emission intensity reduction, which agreed with the findings of Rodríguez and Pena-Boquete, (2017) for Asian Dragons. In other words, the intensive use of labor or intensive growth

of output might reduce the emission intensity. The extensive use of labor could also induce a reduction in emissions intensity, since it reduced the population-labor ratio. The extensive use of labor meant the replacement of labor for energy, leading to lower energy use and lower pollutant emissions. The contribution of trade-related components to emission intensity was not significant for NO_x. As for SO_2, the coefficients for trade components were much lower than other components' coefficients being less than 50%. However, trade openness was expected to lower the emission intensity slightly. In other words, a higher volume of trade might decrease the emission intensity. Emission reducing effect of trade could be assigned to technology transfer, positive spillover effects, productivity gains, and improved managerial skills (Shahbaz *et al.,* 2019). The slight effect of trade openness on emission intensity could be due to the significant fluctuations in trade mainly caused by sanctions. It should be noted that due to the Iran-Iraq war occurred during 1979-1988, the following years (1989-1991) were characterized by reintroducing the production capacities, leading to higher fluctuations in trade-related components. During the study horizon, the industrial output-trade ratio was increased, revealing a lower increase in trade compared to industrial output. The higher values for this ratio were accompanied by a slight increase in emission intensity since the correlation coefficient was only 20%. Accordingly, this could probably show the emissions intensity role of higher industrial output, which agreed with the effect of the inverse industrialization component (industrial output-GDP ratio) with a positive correlation coefficient. In the study horizon, industrialization and its inverse did not show a significant trend and had a slight effect on emission intensity. The related emission coefficient was expected to be closely related to the energy mix or energy structure. For SO_2, the emission coefficient, such as energy structure component, reduced the emission intensity, while for NO_x, the effect of emission coefficient on emission intensity was increasing. The corresponding coefficients were -0.45 and 0.74, respectively. During the study period, electricity use grew much higher than oil products; this could probably provide an opportunity of having lower emissions-energy use ratio i.e., lower emission coefficient. However, for NO_x, the change in energy product composition in favor of natural gas, which was more emission-embodied, played an emission intensity-increasing role. Both emissions-reducing (Zhange *et al.,* 2019) and emission-increasing effects (Rodríguez and Pena-Boquete, 2017; Han *et al.,* 2019) have been reported for this factor.

CO and CO_2 emissions intensity components

As shown in Figs. 8 and 9, a general increasing trend was observed for CO and CO_2 emission intensity, with the emission intensity of CO being slightly stronger. CO emission intensity experienced significant fluctuations, while it exceeded the base year value in most of the study period. Therefore, contrary to NO_x and SO_2 cases, the positive values for correlation coefficients (Fig. 5) meant an increase in emission intensity of the components and vice versa. Similar to the results of NO_x and SO_2, energy structure, population-labor ratio, labor-GDP ratio, inverse industrialization, and trade openness had an emission intensity-dampening effect, while energy intensity, urban per capita output, urbanization and industrial output-trade ratio were expected to raise emission intensity for both CO and CO_2. However, the contribution of these driving factors, except for inverse industrialization, was much higher for CO compared to CO_2, since the correlation coefficients for most of the components of CO were higher than 0.3 in absolute values compared to those of CO_2 which were less than 0.3. This could be due to the fact that CO was mainly emitted from gasoline, while natural gas played a central role in CO_2 emission and gasoline had a slight effect on CO_2 emission (Iran's Energy Balance, 2018). This difference in emission contribution could be attributed to the fact that the increase in these factors more significantly raised the consumption of gasoline rather than natural gas. Most of these variables were closely connected with urbanization and their expansion resulted in higher urban services which had been heavily dependent on gasoline consumption. However, Dong *et al.* (2018) and Han *et al.* (2019) found that urbanization might result in lower carbon intensity. The emission coefficient also contributed to emission intensity, as seen for NO_x. Considering the discussion presented for NO_x and SO_2, the distinguishing aspects for CO were highlighted. The range of fluctuation for the components of CO emissions was broader than that of fluctuations for NO_x and SO_2 (ranging from 100.2 to 113.2 respectively), while the corresponding

ranges for NO_x and SO_2 were 100-102.9 and 99.8-104.2, respectively. In terms of absolute values of correlation coefficients, the values obtained for CO for most components were much lower than those of SO_2. Comparison of these values with the values of NO_x was not straightforward. Although the urban-related components had a more significant role in emission intensity of NO_x and SO_2, their role in CO emission intensity, with correlation coefficients of around 0.3-0.4, was moderate compared to the other components. Despite the significant role of energy intensity in NO_x and SO_2 emissions, its contribution to the emission intensity of CO was slight (0.32). This might be due to the difference in the energy products emitting pollutants. Gas oil plays an essential role in NO_x and SO_2 emissions, while around 97% of CO is emitted from gasoline (Iran's Energy Balance, 2018). CO_2 emission intensity illustrated a strong fluctuation and an insignificant increasing trend. The components with an increasing (decreasing) trend revealed a positive (negative) correlation with the CO_2 emissions intensity. Due to the considerable fluctuations in emission intensity, the correlation coefficients between the CO_2 components and the total emission intensity were lower as compared to the other pollutants. The coefficients were less than 0.11 for four components including energy structure, urban per capita output, urbanization, and population-labor ratio. The corresponding values for other components were lower than 0.34.

Inverse industrialization or GDP-industrial output ratio showed an emission intensity-dampening contribution. As expected, higher GDP-industrial output ratio was associated with lower emission intensity, since the higher ratio was equivalent to higher GDP and resulted in lower emission intensity. The higher ratio could be interpreted as lower industrialization as well. In other words, industrialization might result in more emission intensity. In 2018, around two-thirds of CO_2 was emitted from natural gas. During the study horizon, the natural gas consumption in industrial production increased by 10.8% annually, while the corresponding value for the output was 4.1% (Iran's Energy Balance, 2018), resulting in higher emission intensity. The higher employment and output as well as the

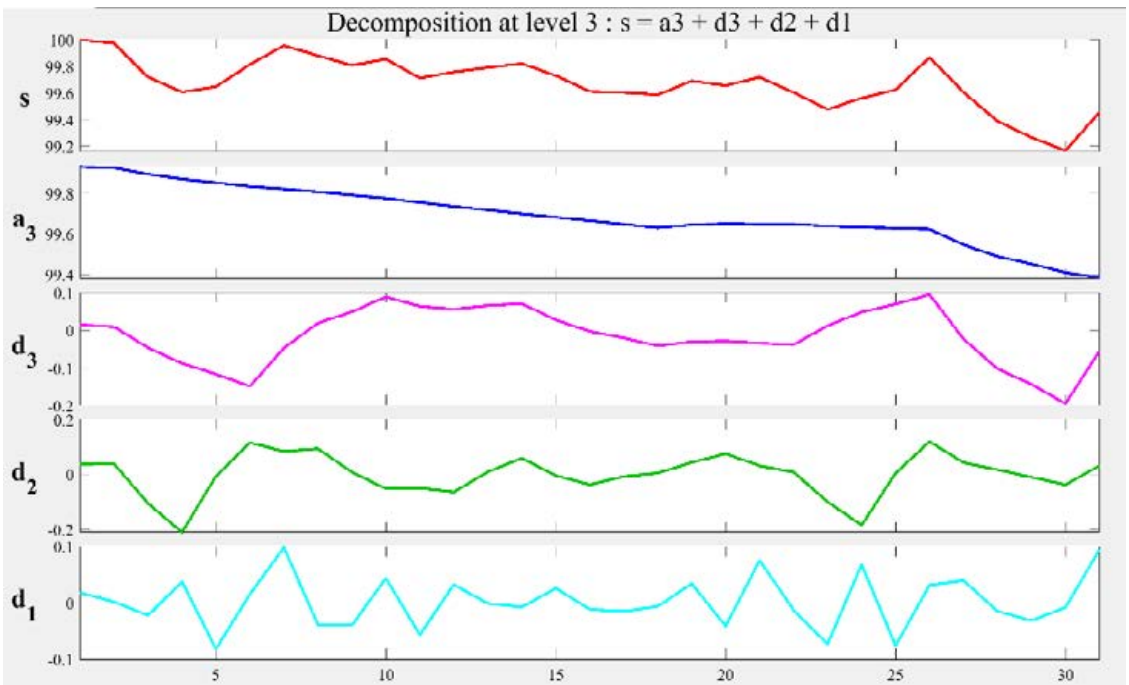

Fig. 10: Decomposition of NO_x time series with 'sym2' wavelet at level 3

Table 2: Training and test forecasting results of the components and total emission intensity

NNs			Components (MLP network)										Total (emissions intensity)		
	criterion	Period	Emission coefficient	Energy structure	Energy intensity	Urban per capita output	Urbanization	Population-labor ratio	Labor-GDP ratio	GDP-industrial output ratio	Industrial output-trade ratio	Trade openness	Based on components	Based on MLP	Based on WNN
NO_x	RMSE	Train	0.0138	0.0045	0.0211	0.0156	0.0021	0.0003	0.0117	0.0007	0.0697	0.0637	-	0.0052	0.0035
		Test	0.0166	0.0085	0.1169	0.0571	0.0056	0.0379	0.1467	0.0533	0.2178	0.1104	0.0803	0.0803	0.0157
	MAPE	Train	0.0114	0.0023	0.0107	0.0065	0.0012	0.0002	0.0088	0.0013	0.0536	0.0263	-	0.0031	0.0026
		Test	0.0137	0.0084	0.1106	0.0440	0.0048	0.0331	0.1425	0.0521	0.1601	0.0897	0.0580	0.0580	0.0154
	MAE	Train	0.0115	0.0016	0.0108	0.0066	0.0013	0.0003	0.0087	0.0003	0.0539	0.0262	-	0.0031	0.0026
		Test	0.0138	0.0081	0.1115	0.0447	0.0049	0.0328	0.1405	0.0522	0.1585	0.0904	0.0575	0.0575	0.0153
	Theil	Train	0.0002	0.0001	0.0001	0.0001	0.0002	0.0004	0.0001	0.0003	0.0004	0.0003	-	0.0002	0.0001
		Test	0.5371	0.3828	0.5799	0.2814	0.2751	0.1914	0.7446	0.2666	0.0011	0.5507	0.0004	0.0004	0.0002
SO_2	RMSE	Train	0.0241	0.0171	0.0376	0.0189	0.0043	0.0286	0.0137	0.0153	0.0895	0.0793	-	0.0732	0.0156
		Test	0.1697	0.0255	0.0270	0.0465	0.0058	0.0421	0.1544	0.1200	0.4122	0.3863	0.0624	0.0844	0.0565
	MAPE	Train	0.0243	0.0051	0.0030	0.0085	0.0015	0.0182	0.0087	0.0077	0.0658	0.0325	-	0.0233	0.0162
		Test	0.1636	0.0234	0.1264	0.0486	0.0049	0.0423	0.1572	0.0853	0.3134	0.3154	0.0645	0.0649	0.0467
	MAE	Train	0.0473	0.0050	0.0130	0.0086	0.0016	0.0181	0.0091	0.0077	0.0559	0.0324	-	0.0213	0.0155
		Test	0.1608	0.0226	0.1268	0.0444	0.0049	0.0421	0.1464	0.0852	0.3125	0.3148	0.0621	0.0625	0.0459
	Theil	Train	0.0031	0.0001	0.0003	0.0002	0.0005	0.0001	0.0003	0.0001	0.0004	0.0003	-	0.0004	0.0002
		Test	0.0010	0.1318	0.1328	0.2288	0.2503	0.0614	0.2771	0.6006	0.0021	0.0019	0.0003	0.0005	0.0003
CO	RMSE	Train	0.0751	0.0235	0.0942	0.0708	0.0068	0.0547	0.0345	0.0434	0.2419	0.3562	-	0.0713	0.0619
		Test	0.1727	0.0308	0.1540	0.0559	0.0059	0.1328	0.7411	0.1834	1.5036	1.4605	0.2046	0.2045	0.1293
	MAPE	Train	0.0360	0.0083	0.0485	0.0435	0.0028	0.0263	0.0122	0.0141	0.1250	0.1408	-	0.0823	0.0469
		Test	0.1860	0.0321	0.1271	0.0498	0.0052	0.1210	0.6820	0.0896	1.4375	1.3174	0.1819	0.1819	0.1006
	MAE	Train	0.0564	0.0064	0.0497	0.0458	0.0029	0.0253	0.0113	0.0146	0.1287	0.1385	-	0.0803	0.0459
		Test	0.1733	0.0306	0.1237	0.0475	0.0053	0.1143	0.6326	0.0861	1.3835	1.2563	0.1867	0.1867	0.1047
	Theil	Train	0.0004	0.0006	0.0005	0.0003	0.0002	0.0003	0.0002	0.0002	0.0012	0.0018	-	0.0005	0.0003
		Test	0.3221	0.6145	0.7500	0.2581	0.2513	0.7018	0.0040	0.0005	0.0076	0.0073	0.0010	0.0010	0.0006
CO_2	RMSE	Train	0.0163	1.6624	5.4318	10.1708	0.0890	0.1362	22.3816	15.8235	10.2472	0.8531	-	0.8058	0.6291
		Test	11.1617	4.3181	42.134	15.5624	1.1408	11.6715	25.0502	65.1245	34.9995	190.728	19.4909	19.4911	4.3061
	MAPE	Train	0.0725	3.6481	1.2534	1.9102	0.0207	0.0412	2.4828	2.1944	1.7376	0.9531	-	0.0912	0.0843
		Test	29.1380	3.7370	9.6207	3.5313	0.3089	9.6047	14.4315	36.0481	16.4338	54.9237	17.9776	17.9769	12.182
	MAE	Train	0.0632	0.9483	3.0834	6.8380	0.0557	0.0851	12.6933	6.0580	4.4450	0.0162	-	0.0831	0.0952
		Test	8.1121	3.9114	35.320	15.5146	1.0162	11.4666	24.3387	55.9126	34.6331	143.911	14.5946	14.5945	3.5334
	Theil	Train	0.0005	0.0149	0.0111	0.0140	0.0002	0.0007	0.0239	0.0250	0.0189	0.0008	-	0.0018	0.0015
		Test	0.1682	0.0201	0.0626	0.0176	0.0017	0.0468	0.0343	0.1439	0.0766	0.5712	0.1638	0.1638	0.0313

stabilized prices addressed by the subsidized energy product consumption have led to energy-dependent industrialization (Farajzadeh, 2018).

An increase in the trade may also lead to lower emission intensity. Greater trade would raise the openness component and decrease the industrial GDP-trade component. Given the correlations (Fig. 5), the increase in trade seemed to induce a reduction in emissions intensity. The corresponding value was around -0.34. Rafig *et al.* (2016) found that trade openness could reduce CO_2 emissions and energy intensity in emerging economies. More exposure to the global interactions may provide opportunities to enjoy modern and clean technology. This channel of trade effect on emission has been specified by Shahbaz *et al.* (2019) as well. Labor productivity component resulted in higher emission intensity of CO_2. Inverse labor productivity showed an intensity-increasing role. In other words, the intensive growth, as suggested by Berndt (1990), can increase the emission intensity since they may substitute away from labor toward energy. However, like other pollutants, the extensive growth via greater use of labor was expected to decrease the emission intensity slightly. Apparently, the extensive use of labor was accompanied by lower use of energy products, revealing a substitution relationship for labor-energy. Emissions coefficient (+0.27) and energy intensity (+0.32) were also positively correlated with the emission intensity of CO_2. The dominant role of natural gas in CO_2 emission was the reason for failure of the energy structure (mix) in affecting the emission intensity. Considering the energy structure, a reduction in emission intensity of CO meant that gasoline was replaced with other energy products, since CO was dominantly emitted by gasoline. It should be noted that over the study period, the composition of energy products changed in favor of natural gas, which was more CO_2-embodied, leading to higher emission factors.

Forecast results

The related data for the emission intensity and its components were divided into training (1980 to 2106) and forecast evaluation (test) subset (2017 and 2018). An architecture with two layers was employed to train the NNs. The Levenberg-Marquardt algorithm and sigmoid function were used as learning algorithm and transfer function, respectively. The 'sym2' wavelet was employed in the WNN training for NO_x, SO_2, and CO prediction, while the 'db2' wavelet was applied for CO_2 prediction, from which the results were obtained in the third resolution. Furthermore, to prepare the data (total case) to feed the NNs, the DWT method was applied in order to decompose the values into approximations and detail components. Fig. 10 illustrates the approximation and detail coefficients. The coefficients extracted using the DWT method were applied as the data for training the WNN.

The results of training and test forecasting of the components and total emission intensity are presented in Table 2. The forecast results were discussed for each pollutant separately. The total (aggregate) emission intensity of each pollutant was forecasted using three methods: the MLP NN model, WNN model, and aggregation of the components. These results are presented in the last three columns of Table 2.

NO_x

The results of NO_x forecast are presented in Table 2. Regarding the accuracy of the forecasts, in the training period, there were slight differences between the components since the RMSE values remained lower than 0.03, except for the trade-related variables (Table 2). MAPE also showed a highly accurate forecast with forecast errors as low as less than 0.1% over the training period. Notably, the prediction error of the training period was slight even for some components including the GDP-industrial output ratio. The significant fluctuations indicated the strong ability of the designed networks to perform predictions over the training horizon. The predictions for the test period also showed a high accuracy; however, the trade-related variables and labor-GDP ratio showed a higher prediction error compared to the other components. In the test period, for most of the components, the prediction error of the last year accounted for most of the test period error, since dramatic changes occurred in the actual values of the last year. Considering the MLP network, during the training period, the total (emission intensity) index showed the highest forecast accuracy. The prediction error presented by the total emission intensity over the test period was much higher than the prediction error in most of the components. This indicated that the decomposition of the total emission intensity to

its components could provide a better opportunity for forecasting the emission intensity more accurately. The WNN was also used for the total emissions intensity index. As presented in the last column of Table 2, the WNN prediction error was lower than the prediction error of the MLP NN. It was also found that predicting the total emission intensity based on the predicted values of the components led to a higher prediction error compared to the predicted values of the WNN. However, considering the low prediction error of less than 0.1%, predicting NO_x emission intensity using the component values was also acceptable.

SO_2

Most of the results obtained from NO_x could be applied to the SO_2 components as well. However, the prediction errors for trade-related variables were higher than those observed for NO_x over the test period (Table 2). Considering the test period, there was a significant difference among the components in terms of prediction error. Trade-related, emission coefficient, and labor-GDP ratio components illustrated a higher prediction error. In the test period, the trade-related variables showed higher prediction errors like those observed for NO_x, whereas the total index showed a lower prediction error, indicating more accurate predictions for other components of SO_2. For most of the components and the total index, the prediction error was observed in the form of an overestimation of the actual values. Similar to NO_x, the low prediction error might allow for predicting the total emission intensity using the values forecasted for the components, since the highest error did not exceed 0.4%.

CO

Table 2 presents the forecast results for CO emission intensity and its components. For CO, also trade variables played an important role in forecast error. The corresponding errors were higher than those obtained for NO_x and SO_2, reaching over 1.3% for the test period. However, the prediction error for other components were similar to those of NO_x and SO_2. Interestingly, even for highly fluctuating components like the GDP-industrial output ratio, the forecasts were presented with high accuracy, indicating the well-designed structure of the networks. While most of the components showed a fluctuating trend (Fig. 8), the forecast accuracy was high for both training and testing periods. It was also found that the second year of the testing period accounted for most of the prediction error. Similar to NO_x and SO_2, the forecasts for the prediction period for the components with lower fluctuations were significantly accurate, indicating that precise forecasts for these components were achievable. The forecast for total emissions intensity based on the predicted components had a high prediction error like NO_x and SO_2.

CO_2

As shown in Fig. 9, the CO_2 emission intensity components showed a fluctuating trend, which made it difficult to design a network with lower prediction error. In terms of forecasting accuracy, CO_2 was different. The prediction errors for other selected pollutants were less than 1.5%, whereas the prediction errors of the test period for 7 components out of 10 were around 10% or higher and around 18% for total emission intensity in MLP network. However, the prediction error over the training period for most of the components was less than 2%. As shown in Fig. 9, there were fluctuations, even for the most years of the training period and for most components, leading to higher prediction errors for the test period. Contrary to the other pollutants, the prediction error for some components of CO_2 was significantly high for the test period. These components were emission coefficient, energy intensity, population-labor ratio, labor-GDP ratio (inverse labor productivity), and GDP-industrial output ratio (inverse industrialization). Among them, emission coefficient and population-labor ratio were forecasted with an extremely high accuracy over the training period, but they showed a high prediction error over the test period. For other components with a higher prediction error, the actual value of the last period seemed to be the strongest fluctuating value over the whole study period. In particular, the comparison of the prediction errors for training and test periods showed that the test period (especially the last year) experienced significant changes. However, even with the current strongly fluctuating test period, prediction errors were acceptable, indicating that the applied networks were well-designed networks. Compared to the MLP NN, the considerable contribution of the WNN was evident as it dampened the prediction error from 18% to 12.2%.

CONCLUSION

Contrary to the current literature that focuses on CO_2 emission, this study examined the emission intensity trend and the driving forces for more pollutants, including NO_x, SO_2, and CO. In terms of the driving forces, to some extent, the emission intensity of CO_2 was found to be different from others. Based on the results, the components such as energy and urban-related variables were mostly involved in forming the trend of emission intensity, while labor, GDP, and trade-related variables, which were mainly and directly affected by the economic variables, accounted for most of the fluctuations in the emission intensity of pollutants. Energy intensity was a driving factor for higher emission intensity, which in turn was affected by a highly subsidizing energy system. It could be claimed that the low price of energy has been resulted in substitution of energy for other production inputs or energy-based industrialization, and higher emission intensity. Thus, removing energy subsidies was recommended from the viewpoint of approaching a less polluted environment. Contrary to the energy intensity, the emission intensity-dampening effect of energy structure occurred through changes in energy product composition indicated a strong chance of achieving a less polluted environment. The results showed that many other factors, such as population, urbanization, and energy-intensive industrialization, could influence the emission intensity. Moreover, both intensive (except for CO_2) and extensive sources of economic growth could reduce the emission intensity of pollutants. This implied that substitution relation might be restricted at some levels, needing to focus on energy use efficiency measures. It was also found that well-organized networks could predict the emission intensity and its components with a high accuracy. The higher prediction error of CO_2 compared to the other pollutants could be attributed to structural changes and significant shocks over the test period. As far as the relevance of the designed NNs was considered, the study horizon included some of the strong fluctuations in the Iranian economy including the Iran-Iraq war and sanctions. Thus, the high accuracy of the forecasts should be considered meantime the strong fluctuations induced by these shocks. It should be noted that the decomposition technique can be used as a tool for a broader extension of the influencing factors far beyond what considered in the present study.

AUTHOR CONTRIBUTIONS

Z. Farajzadeh, the corresponding author, has contributed to designing the paper structure, collecting the data, processing the data, performing the analysis, and writing the manuscript. Also, M. Nematollahi as another corresponding author, has been involved in designing the analysis, performing the simulations, performing the analysis and writing the paper.

ACKNOWLEDGEMENT

This study was supported by the College of Agriculture at Shiraz University [Grant No 99GRC1M84069].

CONFLICT OF INTEREST

The authors declare that they have no known conflict of interests regarding the publication of this manuscript. In addition, the ethical issues, including plagiarism, informed consent, misconduct, data fabrication and/or falsification, double publication and/or submission, and redundancy have been completely observed by the authors.

OPEN ACCESS

©2023 The author(s). This article is licensed under a Creative Commons Attribution 4.0 International License, which permits use, sharing, adaptation, distribution and reproduction in any medium or format, as long as you give appropriate credit to the original author(s) and the source, provide a link to the Creative Commons license, and indicate if changes were made. The images or other third-party material in this article are included in the article's Creative Commons license, unless indicated otherwise in a credit line to the material. If material is not included in the article's Creative Commons license and your intended use is not permitted by statutory regulation or exceeds the permitted use, you will need to obtain permission directly from the copyright holder. To view a copy of this license, visit: http://creativecommons.org/licenses/by/4.0/

PUBLISHER'S NOTE

GJESM Publisher remains neutral with regard to jurisdictional claims in published maps and institutional afflictions.

ABBREVIATIONS

%	Percent
ANN	Artificial neural network
BP	Back-propagation
CH_4	Methane
CO	Carbon monoxide
CO_2	Carbon dioxide
COD	Chemical oxygen demand
DWT	Discrete wavelet transform
FDI	Foreign direct investment
GDP	Gross domestic product
GHGs	Greenhouse gases
GNI	Gross national income
IDA	Index decomposition analysis
LMDI	Log mean Divisia index
MAE	Mean absolute error
MAPE	Mean absolute percentage error
MLP	Multilayer perceptron
N_2O	Nitrous oxide
NNs	Neural networks
NO_x	Nitrogen oxides
OECD	Organization for economic co-operation and development
PPP	Purchasing power parity
RMSE	Root mean squared error
SDA	Structural decomposition analysis
SO_2	Sulphur dioxide
WNNs	Wavelet-based neural networks

REFERENCES

Adom, P.K., (2015). Asymmetric impacts of the determinants of energy intensity in Nigeria. Energy Econ., 49: 570–580 **(11 Pages)**.

Adom, P.K.; Kwakwa, P.A., (2014). Effects of changing trade structure and technical characteristics of the manufacturing sector on energy intensity in Ghana. Renewable Sustainable Energy Rev., 35: 475–483 **(9 Pages)**.

Ang, B.W., (2004). Decomposition analysis for policymaking in energy: Which is the preferred method? Energy Policy, 32: 1131–1139 **(9 Pages).**

Ang, B.W., (2015). LMDI decomposition approach: A guide for implementation. Energy Policy, 86: 233–238 **(6 Pages).**

Ang, B.W.; Zhang, F., (2000). A survey of index decomposition analysis in energy and environmental studies. Energy. 25: 1149–1176 **(8 Pages).**

Berndt, E.R., (1990). Energy use, technical progress and productivity growth: A survey of economic issues. J. Productivity Anal., 2(1): 67–83 **(17 Pages).**

Böhringer, C.; Löschel, A., (2006). Promoting renewable energy in Europe: A hybrid computable general equilibrium approach. The Energy Journal, 27: 135–150 **(16 Pages).**

Central Bank of Iran, (2013). A Yearly Publication.

Cheng, Y.; Wang, Z.; Ye, X.; Wei, Y., (2014). Spatiotemporal dynamics of carbon intensity from energy consumption in China. J. Geogr. Sci., 24: 631–650 **(20 Pages).**

Daubechies, I., (1992). Ten lectures on wavelets, Second ed., SIAM, Philadelphia, PA, USA.

Dogan, E.; Seker, F., (2016). Determinants of CO_2 emissions in the European Union: The role of renewable and non-renewable energy. Renewable Energy, 94: 429-439 **(11 Pages).**

Dong, F.; Yu, B.; Hadachin, T.; Dai, Y.; Wang, Y.; Zhang, S.; Long, R., (2018). Drivers of carbon emission intensity change in China. Resour. Conserv. Recycl., 129: 187-201 **(15 Pages)**.

Farajzadeh, Z., (2018). Emissions tax in Iran: Incorporating pollution disutility in a welfare analysis. J. Cleaner Prod., 186: 618-631 **(14 Pages).**

Farajzadeh, Z.; Nematollahi, M.A., (2018). Energy intensity and its components in Iran: Determinants and trends. Energy Econ., 73: 161-177 **(17 Pages).**

Farajzadeh, Z.; Zhu, X.; Bakhshoodeh, M., (2017). Trade reform in Iran for accession to the World Trade Organization: Analysis of welfare and environmental impacts. Econ. Modelling, 63: 75-85 **(11 Pages).**

Greening, L.A.; Davis, W.B.; Schipper, L.; Khrushch, M., (1997). Comparison of six decomposition methods: application to aggregate energy intensity for manufacturing in 10 OECD countries. Energy Econ., 19: 375 –390 **(16 Pages).**

Han, X.; Cao, T.; Sun, T., (2019). Analysis on the variation rule and influencing factors of energy consumption carbon emission intensity in China's urbanization construction. J. Cleaner Prod., 238: 117958 **(11 Pages).**

Herrerias, M.; Caudros, A.; Orts, V., (2013). Energy intensity and investment ownership across Chinese province. Energy Econ., 36: 286-298 **(13 Pages).**

Holtedahl, P.; Joutz, F.L., (2004). Residential electricity demand in Taiwan. Energy Econ., 26: 201–224 **(24 Pages).**

Hufbauer, G.C.; Schott, J.J.; Annelliott, K.; Muir, J., (2012). Case studies in economic sanction and terrorism.

Iran's Energy Balance, (2018). Deputy of Electricity and Energy Affairs, Ministry of Energy.

Jones, D., (1991). How urbanization affects energy-use in

developing countries. Energy Policy, 19(7): 621-630 **(10 Pages).**

Lau, L.S.; Choong, C.K.; Eng, Y.K., (2014). Investigation of the environmental Kuznets curve for carbon emissions in Malaysia: Do foreign direct investment and trade matter? Energy Policy, 68: 490–497 **(8 Pages).**

Lean, H.H.; Smyth, R., (2010). CO_2 emissions, electricity consumption and output in ASEAN. Appl. Energy, 87: 1858–1864 **(7 Pages).**

Long, X.; Naminse, E.Y.; Du, J.; Zhuang, J., (2015). Nonrenewable energy, renewable energy, carbon dioxide emissions and economic growth in China from 1952 to 2012. Renewable Sustainable Energy Rev., 52: 680-688 **(9 Pages).**

Mallat, S.G., (1989). A theory for multiresolution signal decomposition: The wavelet representation. IEEE Trans. Pattern Anal. Mach. Intel., 11: 674 – 693 **(20 Pages).**

Marrero, G., (2010). Greenhouse gases emissions, growth and energy mix in Europe. Energy Econ., 32: 1356-1363 **(8 Pages).**

Mishra, V.; Smyth, R.; Sharma, S., (2009). The Energy-GDP nexus: Evidence from a panel of Pacific Island countries. Resour. Energy Econ., 31: 210–220 **(11 Pages).**

Naderipour, A.; Abdul-Malek, Z.; Ahmad, N.A,; Kamyab, H.; Ashokkumar, V.; Ngamcharussrivichai, C.; Chelliapan, S., (2020) Efect of COVID-19 virus on reducing GHG emission and increasing energy generated by renewable energy sources: a brief study in Malaysian context. Environ. Technol. Innov., 20: 101151 **(18 Pages)**.

Naderipour, A.; Abdul-Malek, Z.; Arshad, R.; Kamyab, H.; Chelliapan, S.; Ashokkumar, V.; Tavalaei, J., (2021). Assessment of carbon footprint from transportation, electricity, water, and waste generation: towards utilization of renewable energy sources. Clean Technol. Environ. Policy. 23: 183–201 **(18 Pages)**.

Nematollahi, M.A.; Farid, M.; Hematiyan, M.R.; Safavi, A.A., (2012). Crack detection in beam-like structures using a wavelet-based neural network. Proceedings of the Institution of Mechanical Engineers, Part G. Journal of Aerospace Engineering, 226(10): 1243-1254 **(11 Pages)**.

Nematollahi, M.A.; Jamali, B.; Hosseini, M., (2020). Fluid velocity and mass ratio identification of piezoelectric nanotube conveying fluid using inverse analysis. Acta Mech., 231(2): 683-700 **(18 Pages).**

Nematollahi, M.A.; Mousavi Khaneghah, A., (2019). Neural network prediction of friction coefficients of rosemary leaves. J. Food Process Eng., 42(6): 13211 **(12 Pages).**

Pan, X.; Uddin, M.K.; Saima, U.; Jiao, Z.; Han, C., (2019). How do industrialization and trade openness influence energy intensity? Evidence from a path model in case of Bangladesh. Energy Policy, 133: 110916 **(9 Pages).**

Poumanyvong, P.; Kaneko, S., (2010). Does urbanization lead to less energy use and lower CO_2 emissions? A cross-country analysis. Ecol. Econ., 70: 434-444 **(11 Pages).**

Rafiq, S.; Salim, R.; Nielsen, I., (2016). Urbanization, openness, emissions, and energy intensity: A study of increasingly urbanized emerging economies. Energy Econ., 56: 20–28 **(9 Pages).**

Rodríguez, M.; Pena-Boquete, Y., (2017). Carbon intensity changes in the Asian dragons: Lessons for climate policy design. Energy Econ., 66: 17-26 **(10 Pages).**

Rojas R., (1996). Neural Networks-A Systematic Introduction Springer-Verlag. New York.

Sadorrsky, P., (2013). Do urbanization and industrialization affect energy intensity in developing countries. Energy Econ., (37): 52-59 **(8 Pages).**

Statistical Center of Iran (SCI), (2018). National Statistics. https://www.amar.org.ir/english#10291052-national-statistics.

Shahbaz, M.; Gozgor, G.; Adom, P.K.; Hammoudeh, S., (2019). The technical decomposition of carbon emissions and the concerns about FDI and trade openness effects in the United States. Int. Econ., 159: 56-73 **(18 Pages).**

Shahbaz, M.; Khraief, N.; Uddin, G.S.; Ozturk, I., (2014). Environmental Kuznets curve in an open economy: A bounds testing and causality analysis for Tunisia. Renewable Sustain. Energy Rev., 34: 325–336 **(12 Pages).**

Steckel, J.C.; Jakob, M.; Marschinski, R.; Luderer, G., (2011). From carbonization to decarbonization? Past trends and future scenarios for China's CO_2 emissions. Energy Policy, 39: 3443–3455 **(13 Pages).**

Su, B.; Ang, B.W., (2012). Structural decomposition analysis applied to energy and emissions: Some methodological developments. Energy Econ., 34: 177–188 **(12 Pages).**

UNFCCC (United Nations Framework Convention on Climate Change), (2015). UNFCCC Country Brief 2014: Iran.

World Bank, (2004). Islamic Republic of Iran energy-environment Review Policy Note. Report No. 29062-IR. Washington D.C. **(63 Pages).**

World Bank, (2014). Data. IEA Statistics. Energy Use. Washington D.C.

World Bank, (2016). Data. Climate Watch. GHG Emissions. Washington D.C.

World Bank, (2018a). Data. Climate Watch. GHG Emissions. Washington D.C.

World Bank, (2018b). Data. Climate Watch. GHG Emissions. Washington D.C.

World Bank, (2019). Data. World Development Indicators database. Washington D.C.

Xu, X.; Ang, B., (2013). Index decomposition analysis applied to CO_2 emission studies. Ecol. Econ., 93: 313–329 **(17 Pages).**

Zhang, C.; Su, B.; Zhou, K.; Yang, S., (2019). Decomposition analysis of China's CO_2 emissions (2000–2016) and scenario analysis of its carbon intensity targets in 2020 and 2030. Sci. Total Environ., 668: 432-442 **(11 Pages).**

Zhang, P.; Hao, Y., (2020). Rethinking China's environmental target responsibility system: Province-level convergence analysis of pollutant emission intensities in China. J. Cleaner Prod., 242: 118472 **(10 Pages).**

AUTHOR (S) BIOSKETCHES

Farajzadeh, Z., Ph.D., Associate Professor, Department of Agricultural Economics, College of Agriculture, Shiraz University, Shiraz, Iran.
- Email: *zakariafarajzadeh@gmail.com*
- ORCID: 0000-0002-5971-947X
- Web of Science ResearcherID: AGD-1851-2022
- Scopus Author ID: 56708802100
- Homepage: https://agri.shirazu.ac.ir/en/~zakariafarajzadeh

Nematollahi, M.A., Ph.D., Assistant Professor, Department of Biosystems Engineering, College of Agriculture, Shiraz University, Shiraz, Iran.
- Email: *manema@shirazu.ac.ir*
- ORCID: 0000-0001-5780-2723
- Web of Science ResearcherID: W-5769-2018
- Scopus Author ID: 57197262608
- Homepage: https://agri.shirazu.ac.ir/en/~m.nematollahi

HOW TO CITE THIS ARTICLE

Farajzadeh, Z.; Nematollahi , M.A., (2023). Components and predictability of pollutants emission intensity. Global J. Environ., Sci. Manage., 9(2): 241-260.

DOI: 10.22034/gjesm.2023.02.05

url: https://www.gjesm.net/article_255152.html